18

Single Line-to-Ground Fault Detection in Face of Cable Proliferation in Compensated Systems

Wan-Ying Huang, Robert Kaczmarek and Jean-Claude Vannier
Supelec
France

1. Introduction

In case of low ohmic SLG faults in compensated distribution networks, the directional function can be assured by transient relays which compare polarities of zero-sequence charging components at main frequency, either of voltage versus currents on each feeder (Nikander et al., 1995) or of their products on different feeders (Coemans & Maun, 1995). Some difficulties can arise, however, in the presence of violent discharging transients. They grow with inception angle θ, which determines pre-fault values of the faulty line voltage. The discharging currents are absent at θ=0°, but then they reach the charging currents' level when the inception angle is several degrees (Fig. 1), and grow rapidly. The most favorable conditions for generation of important transients are with low resistance fault when it occurs at inception angle 90° in a capacitive network, be it a cabled system or a mixed one composed of cables and lines.

In such conditions, we can expect the extraction of main frequency component out of the charging currents to be more delicate an operation in cables than in lines. The charging components in overhead lines (Lehtonen, 1998) were reported to reach amplitudes 10-15 times the rated frequency amplitude whereas the discharging currents were estimated as several percent of charging components. However, when replacing lines with cables, all the other conditions unchanged, the discharging currents will be more important than the charging ones, with frequency span between them diminishing.

A relevant example comparing amplitudes and frequencies of the main discharging and charging currents (Fig. 2) presents the amplitudes ratio A_{dis}/A_{ch} rising from 0.25 (lines) to 1.5 (cables) and the frequency ratio f_{dis}/f_{ch} diminishing from 11 to 6. The reason of these tendencies is with specific values of zero-sequence capacitances in cables and lines.

Obviously, it is simpler a task to isolate a paramount and somewhat isolated component. The consequence for the transient relays, when applied in capacitive systems, can be an uncertain choice of window and trigger for acquisition and heavy standards on extraction of the relevant charging components.

The disturbing presence of the discharge components can turn into an opportunity to make a correct directional decision. This opportunity is offered by rigorous waveform disposition in initial propagation zone, usually unexplored in distribution systems. However, as the

high frequency acquisition procedures become simpler and cheaper, we are tempted by the travelling wave regime to get directional function.

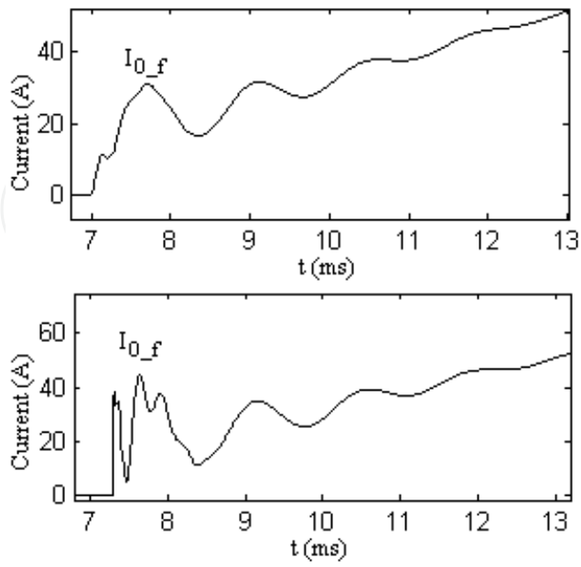

Fig. 1. Initial faulty feeder zero-sequence currents in cables. The discharging currents of higher frequency are superimposed on the charging ones of lower frequency. Upper figure: θ=0°, no discharging components. Bottom: θ=5°, the discharging current's amplitude reach the level of charging components.

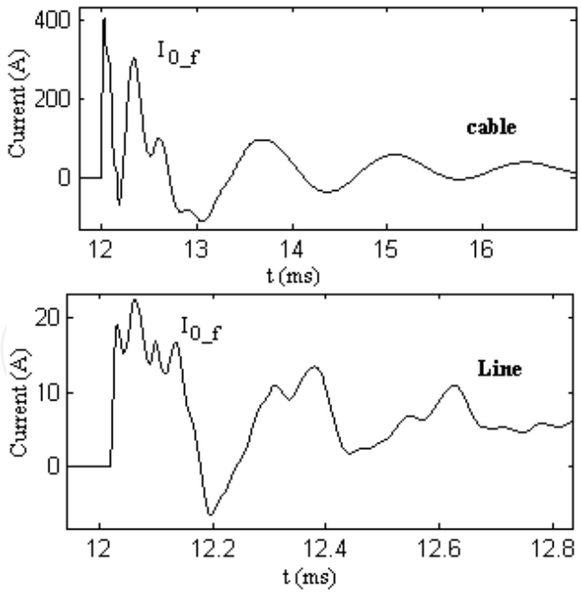

Fig. 2. Faulty feeder zero-sequence currents in cables and lines of the same length and power transfer, with 1Ω fault resistance and 90° inception angle. The discharging components in cables are of higher amplitudes than the charging components and the frequency ratio are different in cables and in lines.

Strong capacitive currents are troublesome also in case of resistive faults, where relays discriminate faulty and sound feeders upon presence of active current component in residual currents. This can be achieved either by comparing signs of projections of zero-sequence currents (Griffel et al., 1997; Welfonder et al., 2000) or looking for phase advance (Bastard et al., 1992; Segui et al., 2001) of the faulty zero-sequence current over the sound ones. However, in steady state the strong capacitive currents diminish this phase advance, with possible inhibition of the discrimination capacities of relays.
Then the way to reestablish these capacities is to exploit data recorded in transient regime, where the apparent phase difference is more important than in the steady state.
Similarly, some difficulties can arise with estimation of fault distance in strongly capacitive systems by exploiting the "main frequency" of charging components (Coemans et al., 1993), or by using the "resonance frequency" of the system (Welfonder et al., 2000), with aid of full zero-positive-negative sequence equation set.
The delicate problem of identification and extraction of the main frequency can be spared when the complete transient waveform is analyzed (Huang & Kaczmarek, 2008), rather than only one of its components. Then the system resistances' damping effect can be taken into account as a relevant parameter, possibly contributing to evaluation of the fault circuit parameters (e.g., with curve fitting).
The transients as they are, generated by faults, carry sufficient information not only for detection of the faulty feeder, but also for evaluation of the fault distance.
The procedures which follow were modeled and simulated in EMTP using frequency dependant parameters.

2. Directional function of discharging currents

We consider a radial network (Fig. 3) with no discontinuities in feeders' impedances. The network is supplied through a transformer with secondary winding grounded through Petersen coil. An SLG fault is modeled as a resistance R_f.
At fault occurrence an initial voltage wave annulling the phase voltage travels along the faulty phase of the faulty feeder with negative amplitude, accompanied by current wave also of negative amplitude. Their shape will be modeled by multiple refractions and reflections from busbar, fault and loads. The faulty phase current arriving on busbar reflects and the resulting current is equally distributed among faulty phases of all the sound feeders. These faulty phase currents impose their waveform upon residuals in each feeder. Consequently, initial currents on the sound feeders will be measured with the same polarity and opposed to the polarity on the faulty feeder.
On each sound feeder, the initial polarity regime will be over with first busbar reflection of wave getting back from loads. Its overall travel time is $2l/v$, with l (feeder's length) and v (wave velocity). This is the time interval where the current on the faulty phase of any sound feeder keeps its initial polarity unchanged. The shortest distance l_{ss} is with the shortest sound feeder and thus we get the duration of the initial polarity $\delta_{ip}=2l_{ss}/v$, where v is the maximal modal velocity.
The parameter $f_{ip}=1/\delta_{ip}$ determines the minimal sampling frequency necessary to get one point in the zone of a rigorous polarity disposition of residual currents.
For example, with the shortest length of a cable feeder being 2km, this frequency can be of 20 – 30 kHz. For practical reasons, the frequency of about 100kHz is to be reckoned with.

In cables the propagation phenomena take place both in cores and sheaths. The fault we refer to is a core-to-sheath (and, eventually, -to-ground) piercing, with sheaths grounded on supply side or on both sides. In each of these cases the traveling waves are very similar and the initial polarity zone clearly exposed (Fig. 4).

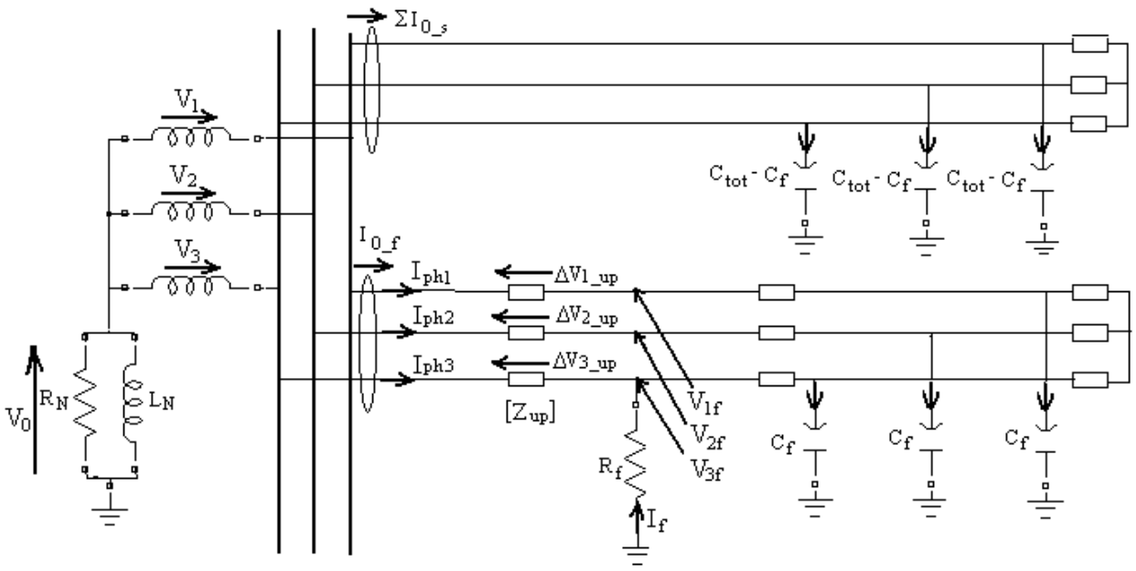

Fig. 3. Phase-to-ground fault in a radial network; all the sound feeders aggregated into one

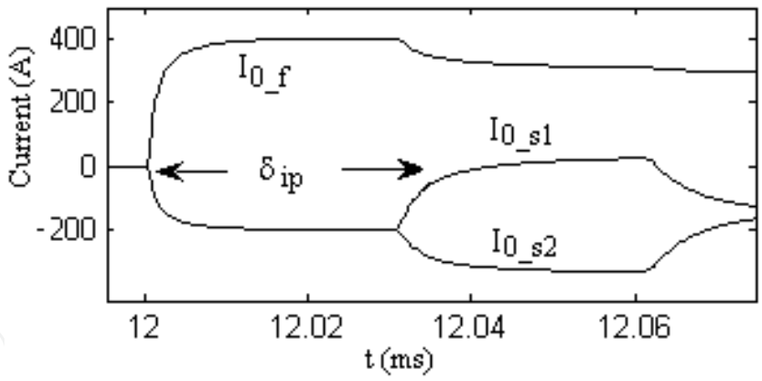

Fig. 4. Initial polarity zone in three feeders' network, zero-sequence currents. The index s is for "sound" and f- for "faulty" feeder

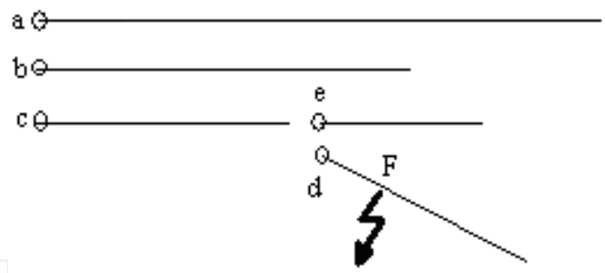

Fig. 5. Phase-to-ground fault F on the feeder "d" in a network with laterals

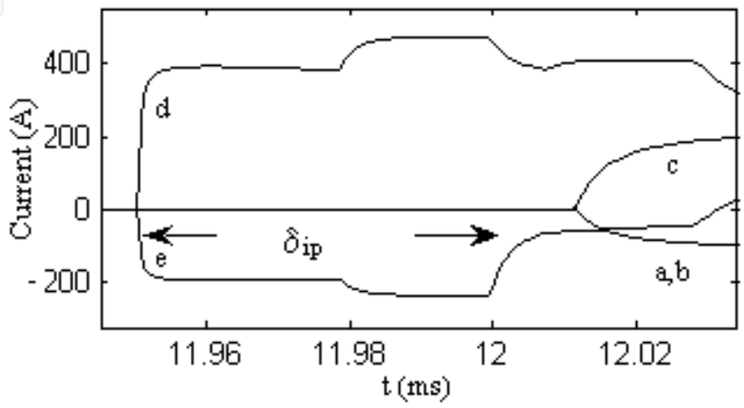

Fig. 6. Residual currents within initial polarity zone in the network of Fig.5

The initial polarity time interval does not depend neither on fault position, nor fault resistance value. If scrutinized on all feeders it can point out from busbar to fault in systems with laterals (Kaczmarek & Huang, 2005). In order to start tracing of the faulty feeder, the initial polarities of residual currents in all busbar connected feeders have to be compared. The beginning of the faulty chain is pointed with a unique sign, called "witness sign", being different from polarity of all the other feeders. Then we follow current sensors on feeders with the same "witness" polarity. The fault is at the end of the chain. This will be illustrated in the case of an SLG fault on the feeder d in a five feeders network (Fig. 5).

The rising current profiles have been recorded first on feeders d and e (Fig. 6). When the traveling waves arrive to busbar, the sign of the current measured on the feeder **c** is different than those measured on the feeders **a** and **b**. The feeder **c,** disclosing the "witness sign", points out to the feeder **d** as the fault location.

All methods based on analysis of traveling waves are highly sensitive to impedance mismatches, what results in severe conditions on their application in distribution networks. Feeders with single tee joints can be analyzed relatively easily, unless the initial polarity zone is too short to be detected. On the contrary, multiple tee joints and joints between cables and lines in mixed systems make the detection problem inextricable in terms of traveling waves' analysis.

3. Directional function of Phase difference

3.1 Principle

The steady state SLG fault regime can be analyzed on equivalent residual circuit (Fig. 7), where V'' is the voltage over a SLG fault emplacement in absence of the fault, I_{0_f} is the zero-sequence current on the faulty feeder, ΣI_{0_s} is the sum of zero-sequence currents on all the sound feeders, and I_N is the neutral point current composed of a resistive and an inductive components.

During permanent fault regime, an active current component is present in zero-sequence current I_{0_f} on the faulty feeder. The resulting phase difference between the faulty and the sound zero-sequence currents I_{0_s} (Fig. 8) is the basis of traditional wattmetric method of detection.

In low capacitive lines the phase advance can be almost 90°, because under the effect of compensation we have (Fig. 7):

$$I_{0\_f} = -I_N - \sum I_{0\_s} = -I_{c\_f} - I_{RN} \tag{1}$$

where the faulty residual I_{0_f} is dominated by its active component I_{RN}.

It is then easy to take direction decision. In cables, however, the faulty feeder capacitive current I_{c_f} dominates the composition of I_{0_f} and diminishes readability of the phase advance, particularly with fault on a long feeder or in case of system over tuning.

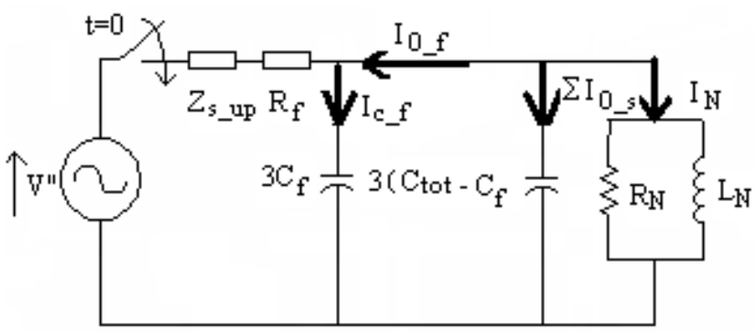

Fig. 7. Equivalent residual circuit of the faulty network on Fig. 3

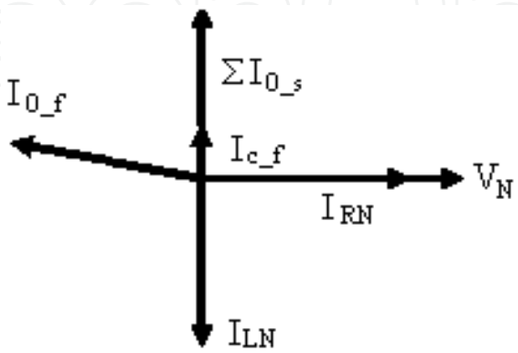

Fig.8. Faulty feeder diagnosis is obvious if there is sufficient phase advance of I_{0_f} over I_{0_s}.

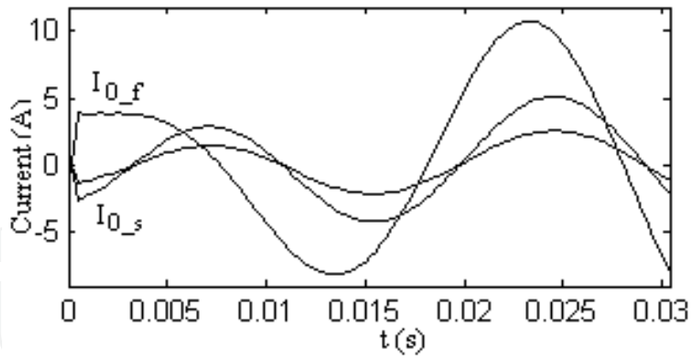

Fig. 9 Faulty and sound current residuals in case of resistive fault, non filtered curves (R_f =1kΩ, θ=90°)

We have simulated a three feeders' cable system of capacitive currents 15A+10A+5A, the fault installed on the 15-A feeder, with 100% tuning and the fault resistance values ranging from 1Ω to 1000Ω. In all cases, the actual phase advance in steady state was less than one sample step at 600Hz sampling frequency, this frequency being used in certain relays.
Fortunately, when the phase advance in steady state becomes undetectable, we can look upon an analogous parameter in transient regime, where it can be much larger.
This is a consequence of the way the transient regime develops, beginning just after the fault inception with phase opposition between faulty and sound current residuals and finishing in steady state with a slight phase advance of the faulty residual over all the sound ones. This development is correlated with evolution of the neutral point current I_N smoothly growing from zero to its permanent value. During the first millisecond after fault inception it can grow very slowly, particularly with resistive faults, because of high values of the neutral point elements L_N and R_N.
On the contrary, the feeders' line-to-ground capacitors C_f and C_s charge and discharge vigorously. During a short time interval, the neutral point current I_N is negligible comparing to capacitive zero-sequence currents.
The latter being under the same charging conditions, the faulty zero-sequence current is initially in phase opposition to the sound feeders zero-sequence currents; see (2):

$$I_{0\_f} = -\left(\sum I_{0\_s}\right) \tag{2}$$

and proceeds toward zero level (Fig. 9) with different polarities. The identification of faulty feeder operates then with aid of following algorithm.

3.2 Algorithm

We detect the slopes of filtered residuals at their first zero crossing after the fault inception. If all but one witness the same slope sign, then we can declare the latter as the faulty one without even controlling its zero crossing:

IF $I_k(t_0)=0$ **for** $k=1\cdots n-1$

AND $\text{sgn}\left(\frac{dI_1}{dt}\right)=\text{sgn}\left(\frac{dI_2}{dt}\right)=\cdots\text{sgn}\left(\frac{dI_{n-1}}{dt}\right)$ **at** $t=t_0$ (3)

THEN *the n[th] feeder is the faulty one*

This is a one shoot procedure, without possibility of verification. On the other hand, it is a conclusive test, as the matter goes about unambiguous identification of slopes' signs.

4. Distance estimation by curve fitting

4.1 Extended Zero-Sequence Circuit (EC) for overhead line

We consider a compensated radial network (Fig. 3) supplied through a delta – star transformer grounded with Petersen coil. A SLG fault through represented by resistance R_f is installed on one of the feeders at the distance l_f from busbar on the phase 3.

The new equivalent circuit which we have developed for fault distance estimation in overhead lines (Huang & Kaczmarek, 2008) (Fig.7), is supplied with the inception voltage

$$V''=-V_3+E_1+E_2 \tag{4}$$

and can easily be calculated from the pre-fault parameters. The correction component E_1 stands for the voltage drop related to the faulted phase load current over the up-stream impedance

$$E_1=Z_{s\_up}I_{l3} \tag{5}$$

where the up-stream self impedance is

$$Z_{s\_up}=\frac{1}{3}\left(Z_{p\_up}+Z_{n\_up}+Z_{0\_up}\right) \tag{6}$$

with Z_{p_up}, Z_{n_up}, and Z_{0_up} as positive, negative and zero sequence impedances. The voltage E_2 stands for the voltage drop related to the sum of the faulted phase load currents of all the n feeders over the internal impedance of sources

$$E_2=Z_{Th}\sum_n I_{l3} \tag{7}$$

Values of inception voltage in case of a 10kV network with total feeders' length 240km, compared to values issued from simulation, are presented in Table 1.

Fault position	0	0.5	1
Calculated inception voltage (16)	5507	5183	4874
Simulated inception voltage	5520	5173	4841
Error [%]	-0.2	+0.2	+0.7

Table 1. Equation-based inception voltage versus simulated one

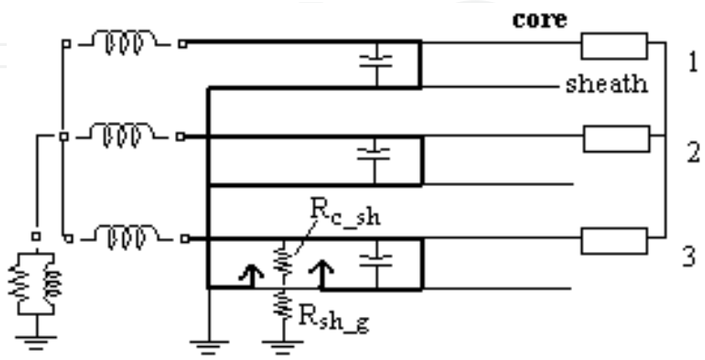

Fig. 10 The core-sheath-ground fault model split into two resistances

4.2 What cables change?

We consider a system with cables grounded on busbar side, the fault being installed (Fig. 10) between core, sheath and ground. The fault evaluating rapidly toward a solid one, the capacitive currents core-sheath choose the core-sheath fault rather than the sheath-ground-neutral point grounding impedance to get back to their original capacitances. The sheath-ground currents being weak, we can ignore the fault resistance sheath-ground.

The simulation confirms independence of currents from the sheath-ground fault resistance, the results being almost the same for one ohm core-sheath resistance R_{c_sh} and different values of the sheath-ground fault resistances R_{sh_g}. Consequently, in our development we ignore the sheath-ground fault resistance.

The corresponding equivalent circuit is apparent to that of overhead lines (Fig.7). The inception voltage V″ (8) is composed of the Thevenin equivalent voltage V_{Th} :

$$V'' = -V_{Th} + E_1 + E_2 \tag{8}$$

the voltage drop E_1 related to the faulted phase load current over the up-stream impedance

$$E_1 = (Z_{c\_up} - Z_{c\_sh\_up}) I_{l3} \tag{9}$$

with Z_{c_up} as up-stream core self impedance and $Z_{c\_sh\_up}$ as up-stream core-sheath mutual impedances. The E_2 related to the sum of the faulted phase load currents of all the n feeders over the internal impedance of sources

$$E_2 = Z_{Th} \sum_n I_{l3} \tag{10}$$

The corresponding up-stream self impedance Z_{s_up} in Fig.7, should be replaced by (Z_{c_up}+Z_{sh_up}-2$Z_{c_sh_up}$) in case of cables with Z_{sh_up} being up-stream sheath self impedance.

Fault position	0	0.5	1
Calculated inception voltage (22)	5591	5427	5263
Simulated inception voltage	5585	5433	5280
Error [%]	+0.1	-0.1	-0.3

Table 2. Equation-based inception voltage versus simulated values

Acc [%]	**EMTP** (reference value) R_f [Ω], l_f [0…1], θ [°]	**EC** R_f [Ω], l_f [0…1], θ [°]	l_f error [% l]
95	1, 0.2, 30	2.3, 0.20, 29	0
100	1, 0.5, 60	4.6, 0.47, 57	-3
105	1, 0.8, 90	12.5, 0.74, 85	-6
95	300, 0.2, 60	306, 0.17, 58	-3
100	300, 0.5, 90	269, 0.68, 87	+18
105	300, 0.8, 30	301, 0.84, 26	+4
95	600, 0.2, 90	584, 0.28, 88	+8
100	600, 0.5, 30	602, 0.52, 27	+2
105	600, 0.8, 60	607, 0.82, 56	+2
95	700, 0.2, 90	649, 0.46, 89	+26
100	700, 0.5, 30	704, 0.52, 27	+2
105	700, 0.8, 60	706, 0.82, 56	+2
95	1000, 0.2, 30	1004,0.21, 28	+1
100	1000, 0.5, 60	1002, 0.52, 57	+2
105	1000, 0.8, 90	986, 0.90, 86	+10
95	3000, 0.2, 60	2983, 0.27, 29	+7
100	3000, 0.5, 90	3074, 0.37, 87	-13
105	3000, 0.8, 30	2993, 0.87, 26	+7

Table 3. Fault on the 22.5km feeder

This way of calculating the inception voltage in cables is satisfactory as show Table 2 with results in a 10kV cable system of total feeders' length 14.5 km.

4.3 Fault distance evaluation by three-parameter fitting

This is a three parameters minimization problem, where the actual fault resistance R_f , fault position l_f, and inception angle θ are given by the equivalent circuit's best fitting curve, with EMTP currents taken for reference data. The EMTP currents are calculated with frequency dependant parameters.

The algorithm has been tested on overhead and cable line radial networks with a SLG fault. In an eight feeders line system of lengths (22.5+24+26+28+32+34+36+37.5)km, at 95…105% tuning, inception angles from 0° to 90°, 10MVA total load and the fault resistance up to 3kΩ we get the fault position with less than 10% mean error in relation to the fault position. Table 3 presents the cases with fault on the feeder of median length.

Acc [%]	**EMTP** (reference value) R_f [Ω], l_f [0…1], θ [°]	**EC** R_f [Ω], l_f [0…1], θ [°]	l_f error [%]
95	1, 0.2, 30	1.0, 0.22, 30	+2
100	1, 0.5, 60	1.2, 0.50, 60	0
105	1, 0.8, 90	2.8, 0.75, 90	-5
95	20, 0.2, 60	20, 0.20, 60	0
100	20, 0.5, 90	23, 0.42, 90	-8
105	20, 0.8, 30	20, 0.80, 30	0
95	50, 0.2, 90	52, 0.12, 90	-8
100	50, 0.2, 30	50, 0.51, 30	+1
105	50, 0.8, 60	50, 0.79, 60	-1
95	200, 0.2, 30	201, 0.17, 30	-3
100	200, 0.5, 60	203, 0.41, 90	-9
105	200, 0.8, 90	203, 0.67, 59	-13

Table 4. Fault on the 6.05km cable feeder

In cables high fault resistances are not relevant, the insulation breakdown being generally definitive, quickly developing to permanent solid fault. In tests on a 3 feeders cable network of feeders' length (3.63; 4.84; 6.05)km, 10MVA total load, at 95…105% tuning and inception angles from 0° to 90°, we get the fault position with average error less than 10% up to R_f=200Ω (Table 4).

5. Conclusion

We think that strong capacitive currents, generating unfavorable conditions for traditional protection relays in compensated systems, can be exploited as carriers of relevant information.

Whenever extremely rapid information is required, we can find it when treating the discharging currents as useful for treatment, at a price of higher sampling frequency. After fault inception we dispose of several tens of microseconds to get the data in wave propagation area. This can make sense in simple distribution systems, with single ramification per feeder and homogenous line impedance.

We can also make useful the presence of strong capacitive currents in permanent fault regime, where these currents occult detection of faulty feeder. In such cases, the diagnosis based on phase advance of the faulty residual current over the sound residuals is better assured when tracing the corresponding apparent phase advance in transient regime.

Both propositions need the current data be centralized; they work on few data points in a very short time span. These drawbacks are price for matching consequences of cable proliferation in resonant grounded distribution networks.

When simulating the fault currents, we usually exploit large possibilities of dedicated packages like EMTP. However, in components in compensated distribution system these currents can be usefully analyzed also with aid of an equivalent circuit, which permits an evaluation of SLG fault distance. We have calculated fault position with several percent average errors, for fault resistance up to 3kΩ in overhead lines or up to 200Ω in cables.

6. References

Bastard, P.; Bertrand, P.; Emura, T. & Meunier, M. (1992). The Technique of Finite-Impulse-Response Filtering Applied to Digital Protection and Control of Medium Voltage Power System. *IEEE Trans. Power Delivery,* Vol. 7, No. 2, (April 1992) pp. 620-626, ISSN 0885-8977

Coemans, J.; Philippot, L. & Maun, J.-C. (1993). Fault distance computation for isolated or compensated networks through electrical transient analysis, *Proceedings of Int. Conf. Power System Transients IPST,* pp. 250-254, 1993

Coemans, J. & Maun, J.-C. (1995). Using the EMTP and the Omicron to design a transients based digital ground-fault relay for isolated or compensated networks, *Proceedings of Int. Conf. Power System Transients IPST*, pp. 270-275, Lisbon, Sept. 1995

Griffel, D.; Harmand, Y.; Leitloff, V. & Bergeal, J. (1997). A new deal for safety and quality on MV networks. *IEEE Trans. Power Delivery,* Vol. 12, No. 4, (Oct. 1997) pp. 1428-1433, ISSN 0885-8977

Huang, W.-Y. & Kaczmarek, R. (2008). Equivalent Circuits for an SLG Fault Distance Evaluation by Curve Fitting in Compensated Distribution Systems. *IEEE Trans. Power Delivery,* Vol. 23, No. 2, (April 2008), pp. 601-608, ISSN 0885-8977

Kaczmarek, R. & Huang, W.-Y. (2005). Directional Function in Distribution Networks through Wave Propagation, *Proceedings of Int. Conf. PowerTech,* pp. , St Petersburg, June 2005

Lehtonen, M. (1998). Fault management in electrical distribution systems. *Final Report of the CIRED working group WG03*, Espoo, Finland, December 1998

Nikander, A.; Lakervi, E. & Suontausta, J. (1995). Applications of transient phenomena during earth faults in electricity distribution networks, *Proceedings of Int. Conf. Energy Management and Power Delivery,* pp. 234-239, Singapore, Nov 1995

Segui, T.; Bertrand, P.; Guillot, M.; Hanchin, P. & Bastard, P. (2001). Fundamental Basis for Distance Relaying with Parametrical Estimation, *IEEE Trans. Power Delivery,* Vol. 16, No. 1, (Jan. 2001) pp. 99-104, ISSN 0885-8977

Welfonder, T.; Leitloff, V.; Feuillet, R. & Vitet, S. (2000). Location strategies ans evaluation of detection algorithms for earth faults in compensated MV distribution systems, *IEEE Trans. Power Delivery,* Vol. 15, No. 4, (Oct. 2000), pp. 1121-1128, ISSN 0885-8977

Fault Detection

Edited by Wei Zhang

ISBN 978-953-307-037-7
Hard cover, 504 pages
Publisher InTech
Published online 01, March, 2010
Published in print edition March, 2010

In this book, a number of innovative fault diagnosis algorithms in recently years are introduced. These methods can detect failures of various types of system effectively, and with a relatively high significance.

InTech Europe
University Campus STeP Ri
Slavka Krautzeka 83/A
51000 Rijeka, Croatia
Phone: +385 (51) 770 447
Fax: +385 (51) 686 166
www.intechopen.com

InTech China
Unit 405, Office Block, Hotel Equatorial Shanghai
No.65, Yan An Road (West), Shanghai, 200040, China
中国上海市延安西路65号上海国际贵都大饭店办公楼405单元
Phone: +86-21-62489820
Fax: +86-21-62489821

IntechOpen